


 CrossMark
 click for updates

 Cite this: *Soft Matter*, 2014, 10, 7034

The role of the hydrophobic phase in the unique rheological properties of saponin adsorption layers†

 Konstantin Golemanov,^a Slavka Tcholakova,^b Nikolai Denkov,^b Eddie Pelan^a and Simeon D. Stoyanov^{*acd}

Saponins are a diverse class of natural, plant derived surfactants, with peculiar molecular structure consisting of a hydrophobic scaffold and one or several hydrophilic oligosaccharide chains. Saponins have strong surface activity and are used as natural emulsifiers and foaming agents in food and beverage, pharmaceutical, ore processing, and other industries. Many saponins form adsorption layers at the air–water interface with extremely high surface elasticity and viscosity. The molecular origin of the observed unique interfacial visco-elasticity of saponin adsorption layers is of great interest from both scientific and application viewpoints. In the current study we demonstrate that the hydrophobic phase in contact with water has a very strong effect on the interfacial properties of saponins and that the interfacial elasticity and viscosity of the saponin adsorption layers decrease in the order: air > hexadecane >> tricaprilyn. The molecular mechanisms behind these trends are analyzed and discussed in the context of the general structure of the surfactant adsorption layers at various nonpolar phase–water interfaces.

Received 20th February 2014

Accepted 6th May 2014

DOI: 10.1039/c4sm00406j

www.rsc.org/softmatter

1. Introduction

The term “saponin” includes a great variety of natural surfactants, found in more than 500 plant species.^{1–3} The saponins are inverted to common surfactants (having a hydrophilic head group and a hydrophobic tail), since they consist of a hydrophobic head group, called aglycone, and one or several hydrophilic oligosaccharide (sugar) chains, connected *via* glycoside bonds to the aglycone. The saponins are classified on the basis of: (i) the type of aglycone (triterpenoid or steroid) and (ii) the number of attached sugar chains. The most common saponins are those with two sugar chains (bidesmosidic saponins) and one sugar chain (monodesmosidic saponins).

Due to their amphiphilic molecular structure, many saponins have strong surface activity. Several authors^{4–11} reported high surface elasticity of saponin adsorption layers at the air–water interface, both in dilatation^{4–6} and shear deformation.^{7–11} These properties are important in the context of saponin

applications as foam and emulsion stabilizers, because the interfacial properties were shown to control many of the dynamic properties of foams and emulsions, such as water drainage, rheological properties, Ostwald ripening, *etc.*^{12–21} In addition, the high shear elasticity of thin layers has become of particular interest recently,^{4–8,22–26} because it is associated with the formation of drops and bubbles with non-Laplacian shapes, periodic wrinkles at interfaces, and other complex phenomena in soft matter systems, which still lack a complete understanding and quantitative description.

In our previous study⁸ we investigated the surface rheological properties of a series of eight triterpenoid and three steroid saponins, with different numbers of oligosaccharide chains. Adsorption layers at the air–water interface, under shear deformations, were studied. All steroid saponins showed no surface shear elasticity and viscosity. In contrast, most of the triterpenoid saponins showed complex visco-elastic behavior with extremely high elastic modulus (up to 1100 mN m^{−1}) and viscosity (130 N s m^{−1}). These values were explained by the formation of densely packed adsorption layers with strong hydrogen bonds between the sugar residues in the neighbouring adsorbed molecules.

In an independent study, Wojciechowski⁶ examined the effect of the hydrophobic phase on the properties of adsorption layers of the saponin extract from one plant (*Quillaja saponaria*). He showed that the surface dilatational elasticity of this triterpenoid saponin decreases in the order: air–water > tetradecane–water > olive oil–water interface. No explanation for the

^aUnilever R&D, Vlaardingen, The Netherlands. E-mail: Simeon.Stoyanov@unilever.com; Fax: +31 10 460 6384; Tel: +31 10 460 6221

^bDepartment of Chemical Engineering, Faculty of Chemistry and Pharmacy, Sofia University, 1 J. Bourchier Ave., 1164 Sofia, Bulgaria

^cLaboratory of Physical Chemistry and Colloid Science, Wageningen University, 6703 HB Wageningen, The Netherlands

^dDepartment of Mechanical Engineering, University College London, Torrington Place, London WC1E 7JE, UK

† Electronic supplementary information (ESI) available. See DOI: 10.1039/c4sm00406j

observed dependence was proposed and the question whether the same trend holds for other saponins and for shear deformation remained open.

Similar effects of the non-polar phase on the rheological properties of adsorption layers of other types of surfactants were reported by several groups.^{27–31} For example, Benjamins *et al.*³⁰ found that the surface dilatational elasticity of adsorption layers of globular proteins decreases in the order: air > tetradecane > triglyceride. The same trend was reported for other proteins by several groups.^{27,30,31} A similar effect was reported by Garofalakis and Murray²⁸ for monolayers of nonionic low-molecular-mass surfactants, when comparing air–water and tetradecane–water interfaces. These results are usually explained in the literature by reduced attraction between the adsorbed surfactant molecules, due to their solvation by the oil molecules at the oil–water interface.

Interestingly, for polymer adsorption layers an opposite effect was reported by Camino *et al.*:²⁹ higher surface elasticity was measured at the triglyceride–water interface, compared to the air–water interface. This result was also explained by the formation of a mixed oil–polymer adsorption layer, which is more visco-elastic, due to the (assumed) strong attraction between the oil molecules and the hydrophobic segments of the polymer molecules.

For all types of surfactant systems (including the mixed surfactant + cosurfactant systems, often used in various applications) one could envisage two possible, conceptually different explanations for the effect of the non-polar phase on the adsorption layer properties. The first mechanism implies a direct intercalation of the oil molecules in between the adsorbed surfactant molecules, thus modifying the molecular interactions within the adsorption layer (Fig. 1A and B). The second mechanism assumes partial dissolution of surfactant molecules into the oily phase (Fig. 1C and D). In both cases, the result is a decreased density of the surfactant adsorption layers and reduced cohesion between the adsorbed molecules (unless a strong specific attraction with oil molecules is assumed, as in ref. 29). The first mechanism is expected to be relevant for globular proteins, due to their low solubility in oil. The second mechanism is expected to be relevant to systems containing low-molecular-mass nonionic surfactants, because of their non-negligible solubility in the oily phase.

For saponins, which are the main subject of the current study, it is entirely unclear in advance which of these mechanisms could occur, due to the lack of essential information about their interfacial rheological properties and their solubility in oil. Furthermore, a given saponin extract usually contains molecules with different numbers of attached saccharide residues, *viz.* such extracts are surfactant mixtures containing molecules with different hydrophilic–lipophilic balances. The oily phase could dissolve most lipophilic components in the saponin extracts, thus effectuating the mechanism illustrated in Fig. 1D. The latter effect could be particularly important also for another very important class of surfactant systems, namely the mixtures of ionic + nonionic surfactants (*e.g.* a mixture of ionic surfactant + fatty alcohol or fatty acid) which are widely used in

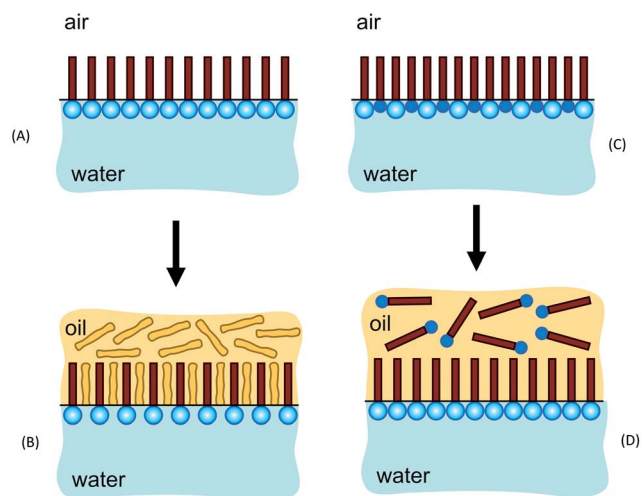


Fig. 1 Schematic presentation of the two main mechanisms of reducing the density and the visco-elasticity of adsorption layers upon their contact with the non-polar liquid (oily) phase. (A) → (B) The oil molecules penetrate between the hydrophobic parts of the adsorbed molecules. (C) → (D) Some fraction of the adsorbed molecules is extracted into the oily phase. In both cases the result is an increased area per molecule and decreased attraction (cohesion) between the molecules in the adsorption layer. Note that the two mechanisms are not alternative, because the extraction of lipophilic surfactants in (D) could be combined with intercalation of oil molecules, as shown in (B).

scientific studies^{32–37} and in various applications to control the surface mobility and dynamic properties of foams.

The main purpose of the current study is to investigate systematically the effect of the hydrophobic phase on the interfacial rheological properties of saponin adsorption layers and to explain the observed trends. We studied a series of eleven saponin extracts,⁸ which differ significantly in their molecular structure – in the type of aglycone and in the number of oligo-saccharide chains. Adsorption layers at the air–water, hexadecane–water and tricapyrylin–water interfaces are compared. Hexadecane is chosen as a representative of typical non-polar oils, whereas tricapyrylin is chosen as a representative of moderately “polar” triglyceride oils, relevant to food and pharmaceutical applications.

We have chosen to compare the shear (not dilatational) rheological properties of the adsorption layers, because the shear deformation does not change the area per molecule. Therefore, this type of measurement emphasizes the role of intermolecular interactions, by excluding their interference with the changes in the area per molecule and the related adsorption–desorption processes, which occur in dilatational surface deformation.

The current study reveals a strong effect of the hydrophobic phase on the interfacial rheological properties of saponin layers. The molecular mechanisms behind the observed trends are explained, and the relevance of the two possible explanations (Fig. 1) to other surfactant systems of general interest is discussed. Besides, the obtained results demonstrate that the saponins can be used as a coherent series of surfactant systems which covers a very wide range of interfacial rheological

properties. Therefore, they are particularly suitable for systematic investigation of the (still elusive) relationship between the interfacial rheological properties and the foaming and emulsifying properties of surfactants.

This article is organized as follows. Section 2 gives brief information on the materials and methods used. Section 3 presents the main results and their discussion. Section 4 summarizes the main conclusions.

2. Materials and methods

2.1. Materials

We studied 11 saponin extracts, obtained from 10 different plants – see ESI† for the molecular structure and the basic physico-chemical properties of the saponins studied. Most of the saponins (8 out of 11) have a triterpenoid hydrophobic backbone – escin (ES), horse chestnut extract (HC), Tea Saponin (TS), Berry Saponin Concentrate (BSC), Sapindin (Sap), *Quillaja* Dry (QD), ginsenosides (GS) and Ayurvedic Saponin Concentrate (ASC). The other saponins – *Tribulus terrestris* (TT), fenusterols (FS) and foamation dry (FD) – have a steroid hydrophobic backbone. A single extract may contain different saponin molecules which share the same aglycone while having different oligosaccharide chains. These chains may differ in number, length or composition (type of sugar residues). Most extracts contained between 25 and 50 wt% saponins. Exceptions were tea saponin, escin, and ginsenosides, which were of higher purity (>80%). Only one of the studied saponins (escin) was a single pure chemical product of Sigma: escin (type II): cat. num. E1378, CAS number 6805-41-0, molecular formula $C_{54}H_{84}O_{23}$. All experiments were performed with solutions containing 0.5 wt% saponin and 10 mM NaCl. Note that all saponin extracts used in this study are highly soluble in water and that the used concentration is well below their solubility limit.

n-Hexadecane with a purity of 99% was obtained from Alfa Aesar (cat. no. A10322; CAS 544-76-3). Tricaprylin (glyceryl tri-octanoate) with a purity of $\geq 99\%$ was obtained from Sigma (cat. no. T9126; CAS 538-23-8). Both oils were used as received. Hexadecane and tricaprylin are abbreviated in the text as “C16” and “3C8”, respectively. The terms “hexadecane–water” and “tricaprylin–water” are abbreviated as “C16–W” and “3C8–W”, respectively.

According to literature data,³⁸ the viscosity of *n*-hexadecane at 20 °C is 3.45 mPa s. The viscosity of tricaprylin at 20 °C was 20.2 mPa s, as measured with a rotational rheometer AR2000ex (TA Instruments), equipped with a cone and plate geometry with a cone radius of 6 cm and a cone angle of 0.3°.

2.2. Methods

The surface rheological properties were characterized using a double-wall ring (DWR)³⁹ attached to an ARG2 rotational rheometer (TA instruments). The rheometer provides information on the angle of rotation of the ring, Ω , and the torque, M , exerted on the ring. From these data and from the geometrical parameters of the setup, one can determine the surface stress and the deformation of the adsorption layer.

In the general case, one has to account for the coupling between the flows in the surface and the sub-surface layers, and the raw data for the torque should be corrected using a numerical procedure.³⁹ However, if the adsorption layer has high surface viscosity, η_s , and the Boussinesq number, $Bo \gg 1$, the analysis is greatly simplified, because the torque originates almost exclusively from the contribution of the surface stress. By definition, the Boussinesq number represents the ratio between the surface and sub-surface drags:⁴⁰

$$Bo = \frac{\eta_s(V/L_S)P_S}{(\eta + \eta_o)(V/L_B)A_S} = \frac{\eta_s}{(\eta + \eta_o)Q} \quad (1)$$

where η is the bulk viscosity of aqueous solution, η_o is the bulk oil viscosity, V is the characteristic flow velocity, and L_S and L_B are the characteristic length-scales over which the surface and sub-surface flows decay. P_S is the perimeter of the geometry in contact with the interface, A_S is the area of the geometry in contact with the bulk phase (solution and oil), and Q is a geometrical parameter. The value of Q for the DWR is ≈ 0.7 mm.³⁹ In most of the experiments presented in the current paper, the Boussinesq number was $Bo \gg 1000$ (viscoelastic layers) or $Bo > 100$ (viscous layers with relatively high η_s) – for these systems the torque on the tool is dominated by the surface stress. In such a case, taking into account that the DWR configuration is a 2D-analog of the double-wall rheometer, one can calculate the surface strain, γ , and surface stress, τ , *via* the relationships:⁴¹

$$\gamma = \frac{\Omega}{\left(\frac{R_2}{R_1}\right)^2 - 1} + \frac{\Omega}{1 - \left(\frac{R_3}{R_4}\right)^2} \quad (2)$$

$$\tau = \frac{M}{2\pi(R_2^2 + R_3^2)} \quad (3)$$

here R_2 and R_3 are the inner and outer radii of the ring, while R_1 and R_4 are the inner and outer radii of the circular channel, respectively.

We subjected the saponin layers to rheological tests in oscillatory (amplitude sweep) and in creep-recovery shear deformation. All experiments were performed at 20 °C. Before each experiment, the studied adsorption layer was pre-sheared for 3 min at a shear rate of 103 s⁻¹ (11 rad s⁻¹). Next, the layer was left to age for a certain period (30 min) and the actual rheological measurements were performed.

In the amplitude sweep test we varied the strain amplitude, γ_A , from 0.01 to 20%, at constant frequency $\nu = 1$ Hz. In the creep-recovery experiments we applied constant stress for a given creep time, $t_{CR} = 100$ s, and afterwards we monitored the relaxation of the deformation for 30 min. Experiments at different torque values were performed.

The experiments showed that the modulus of the viscoelastic saponin layers increased significantly with the time elapsed after the pre-shear of the layer, t_A (for brevity, we call this period “time of layer aging”). To characterize the process of layer aging, we applied continuous oscillations of the adsorption layers for 12 h, at a very small strain amplitude (0.1%) and constant frequency (1 Hz). These measurements allowed us to

monitor the evolution of the viscous and elastic moduli of the layers, as a function of their aging time, t_A .

3. Results and discussion

3.1. Comparison of the rheological response of the adsorption layers formed at various hydrophobic phase–water interfaces

In our previous study,⁸ we showed that saponin extracts with the highest surface elastic moduli at the air–water interface were those of escin, tea saponins and berry saponins, all containing predominantly monodesmosidic triterpenoid saponins. Similarly, a high surface modulus was measured with the ginsenosides extract, containing bidesmosidic triterpenoid saponins with short sugar chains. An intermediate elastic modulus ($\approx 100 \text{ mN m}^{-1}$) and viscosity ($\approx 10 \text{ Pa m s}$) were measured with saponin extracted from *Quillaja saponaria*, containing bidesmosidic triterpenoid saponins with long sugar chains. The other saponin extracts (including all steroid saponins) showed a much lower or negligible surface elasticity at the air–water interface.

In the current study, we first compare all these extracts in creep–recovery experiments, with adsorption layers formed at hexadecane–water and tricaprylin–water interfaces, see Fig. 2. The same experimental conditions are used, as in our previous study⁸ – a torque of $1 \mu\text{N m}$ was applied for 100 s, after 30 min of layer aging. For better structuring the presentation, it is convenient to use the classification from our previous study, where the saponins were divided into several groups, depending on the type of rheological response of the adsorption layers, formed at the air–water interface:

(1) Group EV includes QD, BSC, TS, escin and GS saponins which form layers at the air–water interface with very high surface shear elasticity and viscosity.

From these extracts only QD showed such a high elasticity and viscosity at all the three interfaces studied – see Fig. 2A, where the strain amplitude of the QD elastic adsorption layers is compared at various interfaces.

The adsorption layers of escin and tea saponin extracts exhibit a similar visco-elastic response at air–water and hexadecane–water interfaces, whereas no elasticity and very low viscosity at the tricaprylin–water interface were observed, cf. Fig. 2B and D.

The adsorption layer of GS showed no elasticity and very low viscosity at both the oil–water interfaces studied, see Fig. 2D.

(2) Group V includes HC and SAP which showed a purely viscous response at the air–water interface, with very high shear viscosity (which could be measured directly, because $Bo \gg 1$).

In this group, only sapindin showed high viscosity, $\approx 1.6 \text{ mPa m s}$, at the C16–water interface (Fig. 2C), whereas the layer formed at the tricaprylin–water interface had a much lower viscosity (Fig. 2D). HC showed no measurable elasticity or viscosity for any of the oil–water interfaces studied.

(3) Group LV (low surface viscosity) includes FD, FS, TT and ASC. These extracts show a detectable viscous response at the air–water interface, but the surface viscosity is rather low ($Bo < 30$). All these saponins showed no measurable elasticity or viscosity at any of the oil–water interfaces studied.

From these results we see that the hydrophobic phase has a remarkably high impact on the shear rheological properties of the saponin adsorption layers. The shear visco-elasticity decreases in the order: air–water > hexadecane–water \gg tricaprylin–water interface, which agrees with the trend reported by Wojciechowski⁶ for the dilatational properties of the QD adsorption layer. Therefore, the hydrophobic phase affects significantly both the shear and dilatational surface properties for all the saponins studied.

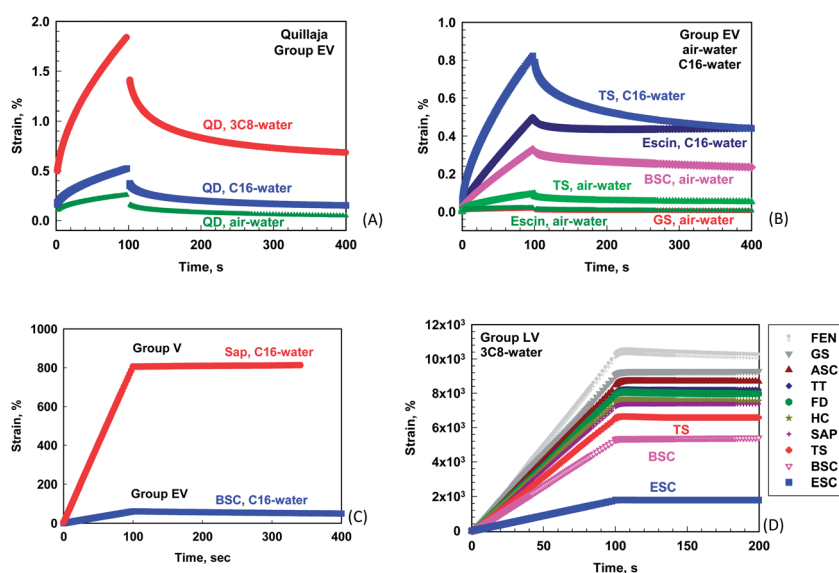


Fig. 2 Creep and relaxation of different saponin adsorption layers: (A, B and C) group EV saponins with elasto–viscous properties of the adsorption layers; (C) group V with measurable surface shear viscosity (Sap); (D) group LV with very low shear surface viscosity. The data for other saponins from this group are given in the ESI.† The experimental conditions are: $t_A = 30 \text{ min}$; $t_{CR} = 100 \text{ s}$; torque $M = 1 \mu\text{N m}$.

As we are interested mostly in the systems with visco-elastic behaviour, below we focus the study on the saponins from group EV.

3.2. Characterization of saponin group EV in creep-recovery experiments

In our previous creep-recovery experiments^{7,8} we showed that the layer compliance is described by a single master curve, *viz.* the rheological parameters are stress-independent, if the applied stress is below a certain critical value, $\tau < \tau_C$. The stress τ_C was similar in value to the critical stress, τ_0 , determined from oscillatory experiments (see Section 3.3). Therefore, both τ_C and τ_0 characterise the stress which leads to disruption of the layer structure.

Previous experiments showed also that the visco-elastic response of the adsorption layers of QD, escin, TS and GS, formed at the air–water interface, could be described very well by the compound Voigt (CV) model.⁴² The mechanical analogue of this model is a combination of one Maxwell and two parallel Kelvin elements, connected sequentially, see Fig. 4C in ref. 8. No simpler rheological model could describe the observed visco-elastic response of these layers, due to the complex shape of the creep-recovery curves.⁷

According to the CV model, the compliance during creep, J_{CR} , is described by the equation:

$$J(t) = \frac{1}{G_0} + \frac{1}{G_1} \left[1 - \exp\left(-\frac{t}{\lambda_1}\right) \right] + \frac{1}{G_2} \left[1 - \exp\left(-\frac{t}{\lambda_2}\right) \right] + \frac{t}{\eta_0} \quad (4)$$

and the compliance during recovery is governed by the expression:

$$J_R(t) = \frac{t_{CR}}{\eta_0} + \frac{1}{G_1} \left[1 - \exp\left(-\frac{t_{CR}}{\lambda_1}\right) \right] \exp\left(-\frac{t}{\lambda_1}\right) + \frac{1}{G_2} \left[1 - \exp\left(-\frac{t_{CR}}{\lambda_2}\right) \right] \exp\left(-\frac{t}{\lambda_2}\right) \quad (5)$$

Here G_0 , η_0 and $\lambda_0 = \eta_0/G_0$ are the elastic modulus, viscosity, and relaxation time of the Maxwell element, while G_i , η_i and $\lambda_i = \eta_i/G_i$ are the respective characteristics of the i -th Kelvin element ($i = 1, 2$).

As explained above, the adsorption layers from the QD extract behave as an elasto-viscous body at all the three interfaces studied (Fig. 2A) and the experimental curves are described very well by the CV model. The adsorption layers of TS at air–water and hexadecane–water interfaces are also described well by the CV model, see Fig. 2B. Interestingly, the escin adsorption layer at the hexadecane–water interface could be described by the simpler Burgers model (BM) which is represented as one Maxwell and one Kelvin elements, connected sequentially.⁴³

The rheological response of the BSC adsorption layer at the air–water interface was described as well by the BM and the layer has surface elasticity. At the air–hexadecane interface, the same layer was better described with the Maxwell model (BM without a Kelvin element) with parameters: $G_0 = 27 \pm 5 \text{ mN m}^{-1}$ and $\eta_0 = 10 \pm 1 \text{ mPa m s}$.

Thus we see that lower elasticity and simpler rheological response are observed in the transition from air–water to hexadecane–water and tricapylin–water interfaces.

The rheological parameters, determined at the different interfaces, are compared in Fig. 3 and Table S2 in the ESI.† For QD layers, one can see that the shear elasticities and viscosities decrease by ≈ 2 times when replacing A–W with the C16–W interface, and further strong reduction is observed for the 3C8–W interface. Even larger effects are observed for the other saponins in this group.

3.3. Characterization of EV adsorption layers in oscillatory experiments

Fig. 4 presents the dependence of the elastic and viscous moduli of different saponins at the C16–W interface, as a function of the strain amplitude, γ_A , at constant frequency (1 Hz). In Fig. 5 we compare these dependences for QD adsorption layers, formed at A–W, C16–W and 3C8–W interfaces.

In all these systems (except for the BSC layer at the C16–W interface) the elastic modulus at low strain amplitudes is much higher than the viscous modulus, *i.e.* these layers are predominantly elastic. In all systems, G' and G'' remain almost constant at low strain amplitudes, up to 1–2%. At a certain strain, the elastic modulus starts to decrease, while the viscous modulus passes through a maximum. These maxima in G'' dependence are explained as arising from the perpetual formation and destruction of the contacts between the structural entities in the slowly deforming layer.^{44,45} In our layers, we expect that G'' increases initially, due to the friction between the sliding domains in the slowly sheared adsorption layers, while the layer structure is disrupted significantly after the maximum G'' , as evidenced by the rapidly decreasing layer elasticity at higher deformation.⁸

One can define several characteristics of the saponin adsorption layers which can be compared and interpreted from physico-chemical and structural viewpoints:

γ_0 is the strain at which the elastic modulus decreases down to 95% of the initial value in the plateau region at $\gamma \rightarrow 0$. We found in ref. 8 that the rheological properties of the adsorption layers are practically the same for all stresses $\tau \leq \tau_0$, where τ_0 is the stress corresponding to γ_0 .

γ_{CR} is the strain at which $G' = G''$ and significant structural changes of the adsorption layers occur. Above the stress τ_{CR} , which corresponds to γ_{CR} , the adsorption layers become fluid and the elastic structure of the layer is lost. At intermediate stresses $\tau_0 < \tau < \tau_{CR}$, the structural changes in the adsorption layer reduce its stiffness, but the main structure of the layer is preserved and one can describe the rheological response by the same rheological model as for the elastic layer, though with reduced values of the rheological parameters.

Fig. 6 presents a comparison of some of these characteristics for the adsorption layers at air–water, hexadecane–water and tricapylin–water interfaces, for the different saponins studied. One can see from Fig. 6A that, for a given saponin, the critical strain γ_{CR} is not affected by the nature of the hydrophobic phase. In contrast, the values of γ_0 are strongly affected by the

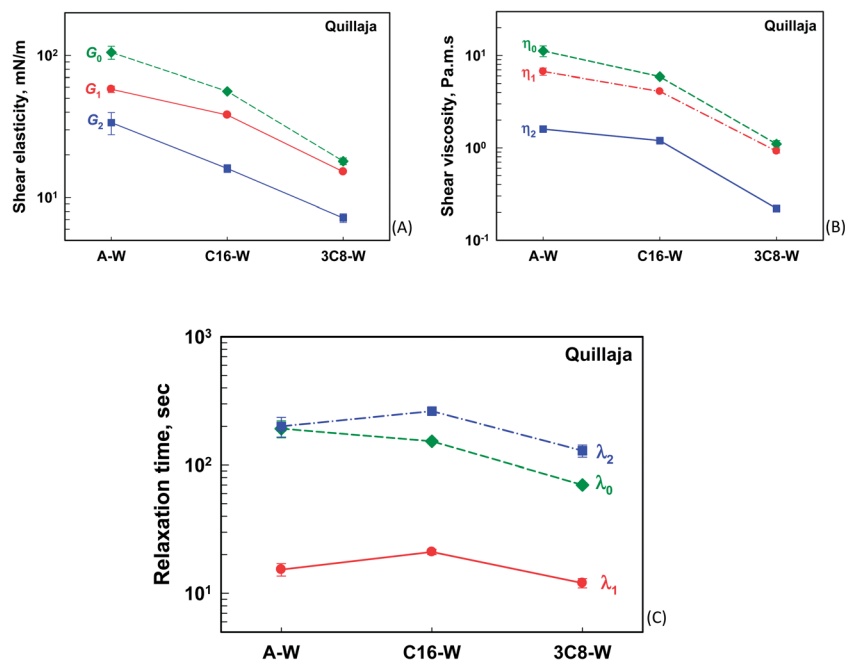


Fig. 3 (A) Surface shear elasticities, (B) surface shear viscosities, and (C) relaxation times for one Maxwell (index 0) and two Kelvin elements (indices 1 and 2) of adsorption layers, formed from *Quillaja* solution at air–water (A–W), hexadecane–water (C16–W) and tricapyrylin–water (3C8–W) interfaces. These values are determined from the best fits to the experimental data with the compound Voigt model. The data are averaged from at least four experiments, performed at least at two different stresses below the critical stress leading to layer fluidization.

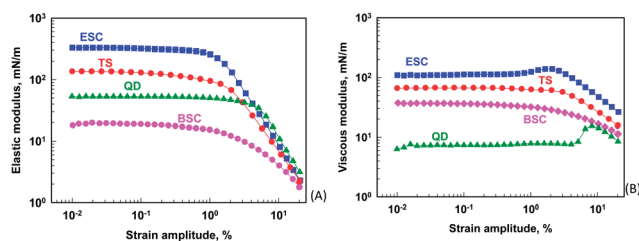


Fig. 4 (A) Elastic modulus and (B) viscous modulus vs. strain amplitude at constant frequency (1 Hz) for saponin adsorption layers, formed at the hexadecane–water interface. The strain amplitude is varied logarithmically from 0.01 to 20%. Layer aging time after pre-shear $t_A = 30$ min.

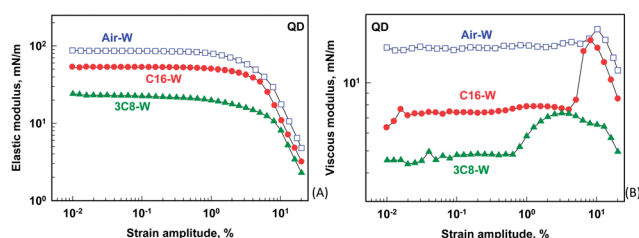


Fig. 5 (A) Elastic modulus and (B) viscous modulus vs. strain amplitude at constant frequency (1 Hz) for adsorption layers of QD at different interfaces (air–water, hexadecane–water, tricapyrylin–water). The strain amplitude is varied logarithmically from 0.01 to 20%. $t_A = 30$ min.

hydrophobic phase. The values of γ_0 are much lower for the C16–W interface, compared to the A–W interface for escin and TS, whereas these are similar for QD. A significant decrease of

γ_0 for QD adsorption layers is observed only for the layers formed at the tricapyrylin–water interface.

The critical stress τ_{CR} , above which the internal structure of the adsorption layers is completely disrupted, is lower for the C16–W interface, compared to the A–W interface for all these saponins, see Fig. 6B. The effect of the hydrophobic phase is even larger for τ_0 (except for QD at the C16–W interface), see the full symbols in Fig. 6B.

In Fig. 7 we summarize the surface elastic and viscous moduli for all saponins, for the three interfaces studied. One can see that the various systems demonstrate a wide variety of behaviours, including highly elastic layers (with much lower viscosity), highly viscous layers (with low elasticity), and layers with negligible visco-elasticity. Such a variety of surface properties provides a unique toolbox for studying the complex relationship between the interfacial rheological properties of the saponin solutions, the peculiar properties of saponin-

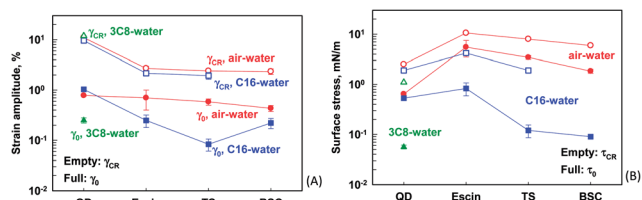


Fig. 6 (A) Strain amplitude at which $G' = 0.95 G''$ ($\gamma \rightarrow 0$) denoted as γ_0 (full symbols), and the strain amplitude at which $G' = G''$ denoted as γ_{CR} (empty points), for saponin adsorption layers formed at air–water (red circles); hexadecane–water (blue squares) and tricapyrylin–water (green triangles) interfaces and the respective stresses (B).

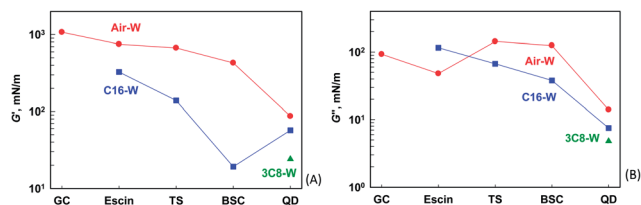
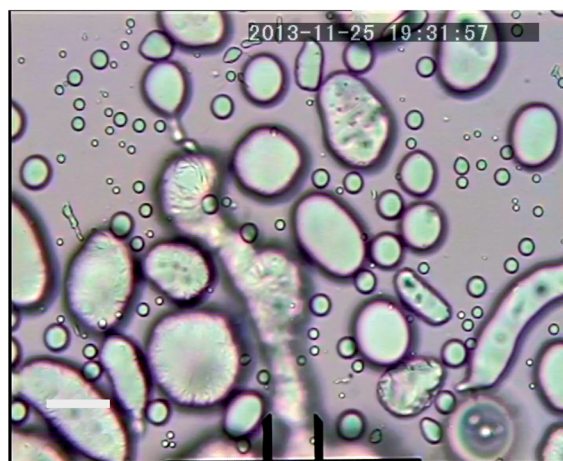


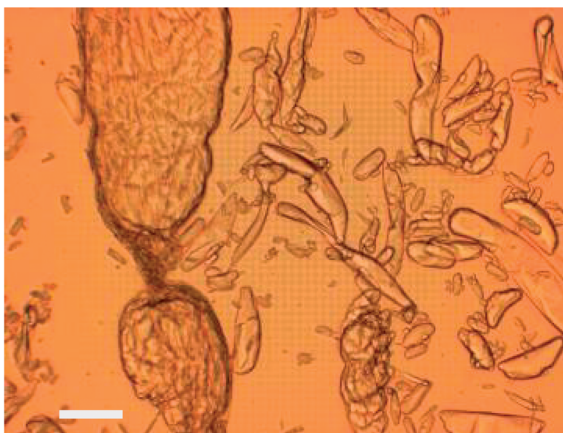
Fig. 7 (A) Elastic modulus upon shear deformation and (B) viscous modulus upon shear deformation of various saponins at various interfaces. Values taken for 0.1% shear deformation (in the linear regime) and 1 s period of oscillations.

stabilized drops and bubbles, and the bulk properties of the respective foams and emulsions.

In ref. 4 we have already demonstrated that *Quillaja* saponin layers made a “skin” on the surface of water droplets with subsequent wrinkling upon large surface contraction (see Fig. 9 in ref. 4). Here, as an additional illustration of the peculiar properties of these systems, we show in Fig. 8 the oil droplets of sunflower oil-in-water emulsion, stabilised with QD and BSC



(A)



(B)

Fig. 8 Micrographs of sunflower oil-in-water emulsion droplets, stabilized by (A) BSC and (B) QD saponins. The droplets have wrinkled surfaces and many are with non-spherical, elongated shape that does not relax for many days, which is indicative for the formation of an elastic adsorption layer with unusual rheological properties at the oil-water interface. The scale bar in the image is 20 μm .

extracts, which have a stable non-spherical shape with wrinkled surface that does not relax for many days. This is a manifestation of the formation of a highly elastic and potentially non-homogeneous surface layer that does not obey the Laplace law of capillarity. The relationship between the interfacial rheological properties and the conditions for the formation of such droplets of peculiar shape is not clear at the moment and we are performing a systematic series of experiments to elucidate this relationship. The analysis of this relationship is complex and goes beyond the scope of the current paper. We could mention now only that the emulsions prepared with the saponin solutions, studied in the current paper, were stable, with a lifetime of days and weeks.

Before entering into the discussion section, we briefly describe the effect of aging (time after pre-shear) of the adsorption layers on their rheological properties. In our previous study⁸ we showed that the properties of the saponin adsorption layers formed at the air-water interface change significantly with aging time for saponins with EV behaviour, see Fig. 8 in ref. 8. These changes reflect a slow rearrangement of the saponin molecules in the adsorption layer, at almost fixed saponin adsorption. For the current study, we performed a similar series of oscillatory experiments in which the surface modulus of the adsorption layers at C16-W and 3C8-W interfaces was measured, as a function of time, at constant frequency (1 Hz) and deformation (0.1%). For all the systems with EV behaviour we observed a steady increase of G' over time which was described well by the bi-exponential function (see Fig. S3 in the ESI[†]):

$$G' = G_0' + G_1'(1 - \exp(-t/t_{R1})) + G_2'(1 - \exp(-t/t_{R2})) \quad (6)$$

where G_0' , G_1' , and G_2' are the surface elastic moduli, while t_{R1} and t_{R2} are the two characteristic times for rearrangement of the saponin molecules in the adsorption layers. From the best fits to the experimental data we determined the values of the parameters which are summarized in Table S3 in the ESI[†].

These results show that t_{R1} and t_{R2} are much longer (scale of hours) than the characteristic relaxation times, λ_i , determined in the creep-relaxation experiments (seconds to several minutes). Therefore, aging includes very slow processes of building and compaction of the domain structure of the adsorption layers. The characteristic times for QD molecules in the adsorption layers at A-W, C16-W and 3C8-W interfaces are all very similar. On the other hand, t_{R1} is about 2 times longer for the escin adsorption layer and more than 4 times longer for TS layers formed at the C16-W interface, compared to the A-W interface. For TS layers, the hydrophobic phase affects also the second characteristic time, t_{R2} . The observed difference between the various saponin extracts is discussed in the following section (3.4).

3.4. Molecular interpretation of the observed effects

Two aspects are considered in the current section from the viewpoint of molecular structure and interactions in the adsorption layer: (1) how the oil phase affects the properties of

the adsorption layers of a given saponin and (2) how the saponin molecular structure affects the layer properties.

Aspect (1) can be considered on the basis of the two possible mechanisms, illustrated in Fig. 1. The possible dissolution of saponin components in the oily phase (Fig. 1C and D) was directly checked by placing 0.5 wt% of each saponin extract (as solid powder) in contact with hexadecane or tricaprylin oil, under stirring with a magnetic stirrer for 1 h. Afterwards, these oily phases were stored overnight for sedimentation of the non-dissolved solid particles and a drop of these oily phases was placed in contact with pure water to measure the oil–water interfacial tension. Any reduction of the interfacial tension below that of the pure oil–water interface would indicate dissolution of some saponin components in the oily phase.

These measurements showed that only TS had noticeable dissolution in hexadecane and BSC – in tricaprylin. For all other saponin extracts, the oil–water interfacial tension was not affected by the oil–saponin contact which is a clear indication for the lack of saponin solubility in the oily phase. Thus we can conclude that, for almost all saponin systems studied, the observed lower surface elasticity and viscosity could be explained only by intercalation of oil molecules between the adsorbed saponin molecules, Fig. 1A and B.

The experimental results indicate that the intercalation of hexadecane molecules weakens the interactions between the saponin molecules in the adsorption layers (Fig. 9A and B), but without destroying the layer structure and the layers preserve their visco-elastic nature. The observed effect of tricaprylin is more dramatic, probably because the polar heads of the triglyceride molecules tend to be in contact with the water molecules at the interface, as shown in Fig. 9C. Such deep penetration of the bulky tricaprylin molecules inside the adsorption layer should lead to much larger spacing between

the adsorbed saponin molecules and strongly reduced interactions, just as observed experimentally. Indeed, the comparison of the surface tension isotherms of tea saponin at air–water and tricaprylin–water interfaces showed that the slope of the dependence of the interfacial tension *vs.* logarithm of surfactant concentration is about 50% larger for the air–water interface. According to the Gibbs adsorption equation, this larger slope corresponds to larger area per molecule in the adsorption layer at the oil–water interface.

Only for TS at the hexadecane–water interface and for BSC at the tricaprylin–water interface we could not determine unambiguously which of the two mechanisms is dominant – the observed solubility of these saponins in the oil phase keeps the possibility open that the mechanism of partial dissolution shown in Fig. 1D could be also important, besides the intercalation mechanism shown in Fig. 1B.

Aspect (2) concerns the effect of saponin molecular structure on the layer rheological properties. As explained in our previous study,⁸ the layers of escin, TS and QD exhibit high visco-elasticity, most probably due to formation of strong intermolecular hydrogen bonds between the sugar chains of the nicely packed neighbouring molecules in the adsorption layers. The latter explanation is supported by the fact that the elastic properties of these layers are lost when a chaotropic agent urea (known to disrupt the hydrogen bonds) is placed in the aqueous phase, see Fig. 10.

As discussed in ref. 7 and 8, the monodesmosidic escin and tea saponins (with one oligosaccharide chain) are packed at the air–water interface in side-on configuration (Fig. 9A) with an area per molecule of around 0.5 nm², whereas the bidesmosidic QD is in a lay-on configuration (Fig. 9D) with an area per molecule of ≈ 1 nm². The current study shows that the monodesmosidic saponins had a much lower visco-elastic modulus at

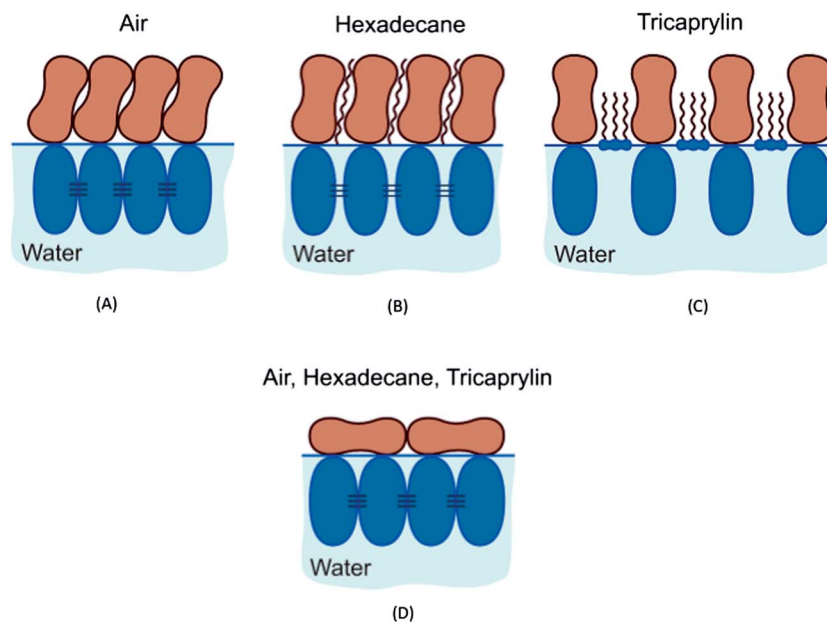


Fig. 9 Schematic presentation of the structure of the saponin adsorption layers for (A–C) monodesmosidic saponins escin and TS, and (D) bidesmosidic saponin QD at various interfaces.

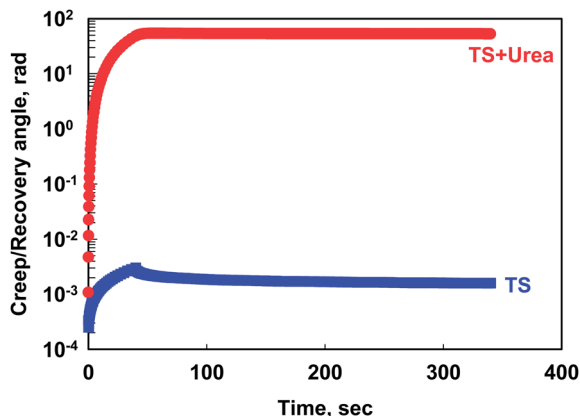


Fig. 10 Creep and relaxation curves for adsorption layers of tea saponin (TS) at the air–water interface, with 4 M urea and without urea in the aqueous phase. The chaotropic agent urea breaks the hydrogen bonds and the layer is fluidized, as evidenced by the large creep in the presence of urea (red curve). The conditions of the experiment are $t_A = 30$ min; $t_{CR} = 100$ s; torque $M = 1 \mu\text{N m}$.

the oil–water interface, as compared to the air–water interface. In contrast, the modulus of the bidesmosidic QD layer was only moderately lower for the hexadecane–water interface and still significant for the tricapyrylin–water interface. All relaxation times for QD are weakly affected by the hydrophobic phase which was not the case for the other saponins. Thus we can see that the lay-on configuration of QD saponins is significantly less affected by the nature of the hydrophobic phase. Apparently, the two sugar chains attached to the aglycone of the QD molecules act as “anchors” and fix better the QD molecules to the interface, thus reducing the effect of the oil molecules.

At the end, let us discuss briefly the relevance of the mechanisms shown in Fig. 1 to the other main systems mentioned in the Introduction. Proteins are typically insoluble in oil phases. Therefore, the intercalation of oil molecules between the adsorbed protein molecules is the only possible mechanism for these systems (Fig. 1B).

For the mixtures of ionic surfactant + fatty acids, very high surface dilatational moduli were reported for the air–water interface, of the order of $100\text{--}300 \text{ mN m}^{-1}$. For the current study we measured the surface modulus for the same systems (by the oscillating drop method) at hexadecane–water and tricapyryline–water interfaces and found that the surface moduli were strongly reduced to $<5 \text{ mN m}^{-1}$. The fatty acids used as cosurfactants in these systems are known to have rather high solubility in oily phases. Therefore, for these systems we can see that both mechanisms are operative, as shown in Fig. 1, because the extraction of the cosurfactant molecules is accompanied also by intercalation of oil molecules between the chains of the main surfactant. The latter assumption is supported by measurements of other authors²⁸ which showed that the area per molecule of surfactants is usually larger at oil–water interfaces, as compared to the air–water interface. Similar is the mechanistic explanation for the other types of nonionic cosurfactant (dodecanol, tetradecanol) widely used in foam studies and applications.

4. Main results and conclusions

In this article we compared the shear rheological properties of saponin adsorption layers at air–water, hexadecane–water and tricapyrylin–water interfaces. Eight triterpenoid and three steroid saponins are compared. The main conclusions could be summarized as follows:

In all experiments, the steroid saponins (TT, FS and FD) had very low shear interfacial viscosity and no measurable elasticity.

Three of the triterpenoid saponins showed visco-elastic behaviour at the hexadecane–water interface. These were two monodesmosidic saponins (TS and ESC) and one bidesmosidic saponin (QD), all of which share the same aglycone (triterpenoid, oleanane type). The obtained results show that the layers of the monodesmosidic saponins are affected to a much higher degree by their contact with hexadecane and tricapyrylin, as compared to the bidesmosidic saponin with the same aglycone. The oil molecules get intercalated in the adsorption layer and perturb strongly the packing of the monodesmosidic molecules at the interface, thus weakening the interactions between them (Fig. 9A–C). In contrast, the orientation of the bidesmosidic molecules at the interface is better fixed by the two oligosaccharide chains in the molecules – as a result, the layer structure and rheological behaviour are less dependent on the nature of the non-aqueous phase (Fig. 9D).

The possible mechanisms behind the observed trends are discussed, Fig. 1 and 9, and a comparison with other systems forming visco-elastic adsorption layers (proteins, mixtures of ionic + nonionic surfactants) was performed and is discussed in Section 3.4.

The observed variety of interfacial rheological properties (see Fig. 7) shows that the saponins present a unique series of structurally similar molecular systems which cover all major types of surface visco-elastic behaviour. This variety of properties makes saponins particularly suitable for studying the intriguing and still poorly understood relationship between the interfacial rheological properties and the properties of drops and bubbles, emulsions and foams (*e.g.* Fig. 8).

Acknowledgements

The authors are grateful to Unilever R&D Vlaardingen, FP7 Project Beyond Everest, COST Actions FA1001 and MP1106 for the support. K.G. is grateful to the Marie Curie Intra-European fellowship program. The measurements of the dilatational modulus of SLES + CAPB + myristic acid by the oscillating drop method and of the saponin solubility characterization were performed by Ms Nevena Borisova. The authors are particularly grateful to the referees who made several useful suggestions for improving the manuscript.

References

- 1 K. Hostettmann and A. Marston, *Saponins*, Cambridge University Press, New York, 1995.

- 2 J.-P. Vincken, L. Heng, A. De Groot and H. Gruppen, Saponins, classification and occurrence in the plant kingdom, *Phytochemistry*, 2007, **68**, 275.
- 3 Q. Guglu-Ustundag and G. Mazza, Saponins: Properties, applications and processing, *Crit. Rev. Food Sci. Nutr.*, 2007, **47**, 231–258.
- 4 R. Stanimirova, K. Marinova, S. Tcholakova, N. D. Denkov, S. Stoyanov and E. Pelan, Surface Rheology of Saponin Adsorption Layers, *Langmuir*, 2011, **27**, 12486–12498.
- 5 K. Wojciechowski, M. Orczyk, K. Marcinkowski, T. Kobiela, M. Trapp, T. Gutberlet and T. Geue, Effect of hydration of sugar groups on adsorption of *Quillaja* Bark saponin at air/water and Si/water interfaces, *Colloids Surf., B*, 2014, **117**, 60.
- 6 K. Wojciechowski, Surface Activity Of Saponin From *Quillaja* Bark At The Air/Water And Oil/Water Interfaces, *Colloids Surf., B*, 2013, **108**, 95.
- 7 K. Golemanov, S. Tcholakova, N. D. Denkov, E. Pelan and S. Stoyanov, Surface shear rheology of saponins, *Langmuir*, 2012, **28**, 12071.
- 8 K. Golemanov, S. Tcholakova, N. D. Denkov, E. Pelan and S. D. Stoyanov, Remarkably high surface visco-elasticity of adsorption layers of triterpenoid saponins, *Soft Matter*, 2013, **9**, 5738–5752.
- 9 S. A. Shorter, On Surface Separation from solutions of Saponin Peptone, and Albumin, *Phil. Mag.*, 1909, **17**, 560–563.
- 10 P. Joos, R. Vochten and R. Ruysen, The Surface Shear Viscosity of Mixed Monolayers Interaction Between Cholesterol and Digitonin, *Bull. Soc. Chim. Belg.*, 1967, **76**, 601.
- 11 T. B. J. Blijdenstein, P. W. N. de Groot and S. D. Stoyanov, On the link between foam coarsening and surface rheology: Why hydrophobins are so different, *Soft Matter*, 2010, **6**, 1799–1808.
- 12 E. Dickinson, B. S. Murray and G. Stainsby, Coalescence Stability of Emulsion-sized Droplets at Planar Oil–Water Interface and the Relationship to Protein Film Surface Rheology, *J. Chem. Soc., Faraday Trans.*, 1998, **84**, 871.
- 13 S. Mun and J. McClements, Influence of Interfacial Characteristics on Ostwald Ripening in Hydrocarbon Oil-in-Water Emulsions, *Langmuir*, 2006, **22**, 1551.
- 14 M. B. J. Meinders, W. Kloek and T. van Vliet, Effect of Surface Elasticity on Ostwald Ripening in Emulsions, *Langmuir*, 2001, **17**, 3923.
- 15 S. Tcholakova, Z. Mitrova, K. Golemanov, N. D. Denkov, M. Vethamuthu and K. P. Ananthpadmanabhan, Control of bubble Ostwald ripening in foams by using surfactant mixtures, *Langmuir*, 2011, **27**, 14807–14819.
- 16 D. Langevin, Influence of interfacial rheology on foam and emulsion properties, *Adv. Colloid Interface Sci.*, 2000, **88**, 209–222.
- 17 D. Langevin, Aqueous foams: A field of investigation at the Frontier between chemistry and physics, *ChemPhysChem*, 2008, **9**, 510–522.
- 18 S. P. L. Marze, A. Saint-Jalmes and D. Langevin, Protein and surfactant foams: Linear rheology and dilatancy effect, *Colloids Surf., A*, 2005, **263**, 121–128.
- 19 A. Saint-Jalmes, Y. Zhang and D. Langevin, Quantitative description of foam drainage: Transitions with surface mobility, *Eur. Phys. J. E: Soft Matter Biol. Phys.*, 2004, **15**, 53–60.
- 20 A. Saint-Jalmes and D. Langevin, Time evolution of aqueous foams: Drainage and coarsening, *J. Phys.: Condens. Matter*, 2002, **14**, 9397–9412.
- 21 D. Y. Zang, E. Rio, G. Delon, D. Langevin, B. Wei and B. P. Binks, Influence of the contact angle of silica nanoparticles at the air–water interface on the mechanical properties of the layers composed of these particles, *Mol. Phys.*, 2011, **109**, 1057–1066.
- 22 N. A. Alexandrov, K. G. Marinova, T. D. Gurkov, K. D. Danov, P. A. Kralchevsky, S. D. Stoyanov, T. B. J. Blijdenstein, E. Pelan and A. Lips, Interfacial layers from the protein HFBII hydrophobin: Dynamic surface tension, dilatational elasticity and relaxation times, *J. Colloid Interface Sci.*, 2013, **376**, 296–306.
- 23 S. Knoche, D. Vella, E. Aumaitre, P. Degen, H. Rehage, P. Cicuta and J. Kierfeld, Elastometry of deflated capsules: Elastic moduli from shape and wrinkle analysis, *Langmuir*, 2013, **29**, 12463–12471.
- 24 P. Erni, H. A. Jerri, K. Wong and A. Parker, Interfacial viscoelasticity controls buckling, wrinkling and arrest in emulsion drops undergoing mass transfer, *Soft Matter*, 2012, **8**, 6958–6967.
- 25 E. Aumaitre, S. Knoche, P. Cicuta and D. Vella, Wrinkling in the deflation of elastic bubbles, *Eur. Phys. J. E: Soft Matter Biol. Phys.*, 2013, **36**, 22.
- 26 A. B. Subramaniam, M. Abkarian, L. Mahadevan and H. A. Stone, Colloid science: Non-spherical bubbles, *Nature*, 2005, **438**, 930.
- 27 L. Seta, N. Baldino, D. Gabriele, F. R. Lupi and B. de Cindio, The effect of surfactant type on the rheology of ovalbumin layers at the air/water and oil/water interfaces, *Food Hydrocolloids*, 2012, **29**, 247–257.
- 28 G. Garofalakis and B. S. Murray, Surface pressure isotherms, dilatational rheology, and Brewster angle microscopy of insoluble monolayers of sugar monoesters, *Langmuir*, 2002, **18**, 4765–4774.
- 29 N. A. Camino, O. E. Perez, C. C. Sanchez, J. M. R. Patino and A. M. R. Pilosof, Hydroxypropylmethylcellulose surface activity at equilibrium and adsorption dynamics at the air–water and oil–water interfaces, *Food Hydrocolloids*, 2009, **23**, 2359–2368.
- 30 J. Benjamins, J. Lyklema and E. H. Lucassen-Reynders, Compression/expansion rheology of oil/water interfaces with adsorbed proteins. Comparison with the air/water surface, *Langmuir*, 2006, **22**, 6181–6188.
- 31 R. Wustneck, B. Moser and G. Muschiolik, Interfacial dilatational behavior of adsorbed β -lactoglobulin layers at the different fluid interfaces, *Colloids Surf., B*, 1999, **15**, 263–273.
- 32 S. A. Koehler, S. Hilgenfeldt and H. A. Stone, Liquid Flow through Aqueous Foams: The Node-Dominated Foam Drainage Equation, *Phys. Rev. Lett.*, 1999, **82**, 4232.

- 33 K. Golemanov, N. D. Denkov, S. Tcholakova, M. Vethamuthu and A. Lips, Surfactant mixtures for control of bubble surface mobility in foam studies, *Langmuir*, 2008, **24**, 9956.
- 34 N. Adami, S. Dorbolo and H. Caps, Single thermal plume in locally heated vertical soap films, *Phys. Rev. E: Stat., Nonlinear, Soft Matter Phys.*, 2011, **84**, 046316.
- 35 A. L. Biance, A. Delbos and O. Pitois, How topological rearrangements and liquid fraction control liquid foam stability, *Phys. Rev. Lett.*, 2011, **106**, 068301.
- 36 B. Dollet, Local description of the two-dimensional flow of foam through a contraction, *J. Rheol.*, 2010, **54**, 741.
- 37 Z. Mitrinova, S. Tcholakova, K. Golemanov, N. D. Denkov, M. Vethamuthu and K. P. Ananthapadmanabhan, Surface and foam properties of SLES + CAPB + fatty acid mixtures: Effect of pH for C12–C16 acids, *Colloids Surf., A*, 2013, **438**, 186–198.
- 38 E. F. Cooper and A. A.-F. Astour, Densities and Kinematic Viscosities of some C₆–C₁₆ *n*-Alkane Binary Liquid Systems at 293.15 K, *J. Chem. Eng. Data*, 1991, **36**, 285.
- 39 S. Vandebril, A. Franc, G. G. Fuller, P. Moldenaers and J. Vermant, A double wall-ring geometry for interfacial shear rheometry, *Rheol. Acta*, 2010, **49**, 131.
- 40 D. A. Edwards, H. Brenner and D. T. Wasan, *Interfacial Transport Processes and Rheology*, Butterworth-Heinemann, Boston, 1991.
- 41 A. Franck, S. Vandebril, J. Vermant and G. Fuller, *Double wall ring geometry to measure interfacial rheological properties*, 5th International Symposium on Food Rheology and Structure, Zurich, Switzerland, 2008.
- 42 F. Mainardi, *Fractional Calculus and Waves in Linear Viscoelasticity: An Introduction to Mathematical Models*, Imperial College Press, London, 2010.
- 43 T. G. Mezger, *The Rheology Handbook*, Vincentz Network, Hannover, 2nd edn, 2006.
- 44 K. Hyun, M. Wilhelm, C. O. Klein, K. S. Cho, J. G. Nam, K. H. Ahn, S. J. Lee, R. H. Ewoldt and G. H. McKinley, A review of nonlinear oscillatory shear tests: Analysis and application of large amplitude oscillatory shear (LAOS), *Prog. Polym. Sci.*, 2011, **36**, 1697–1753.
- 45 M. Parthasarathy and D. J. J. Klingenberg, Large amplitude oscillatory shear of ER suspensions, *J. Non-Newtonian Fluid Mech.*, 1999, **81**, 83–104.